Bandwidth-Enhanced PAM-4 Transmissions using Polarization Modulation and Direct Detection with a Tunable Frequency Range

Siming Liu, Peng-Chun Peng, Long Huang, Chin-Wei Hsu, Huiping Tian, and Gee-Kung Chang, *Fellow, IEEE, Fellow, OSA*

***Abstract*—We propose a polarization-modulation and direct-detection (PolM-DD) bandwidth-enhanced PAM-4 transmission system with a tunable frequency range and demonstrate, for the first time, its performance after transmissions through a standard single mode fiber (SSMF). By adjusting the polarization angle between one principal axis of the PolM and polarizer, the frequency notch, caused by the spectral dispersion inherent in SSMF, can be shifted to higher frequencies. As a consequence, the available 3-dB bandwidth at the baseband is much more enhanced than it would be in the traditional case of an intensity-modulation and direct-detection (IM-DD) system. Since the output of PolM modulation module are intensity modulated signals with a tunable chirp, the system is free of polarization-mode dispersion (PMD). From the analysis in this paper, we conclude that under ideal conditions, the PolM-DD system gains approximately 41.4% in bandwidth over its counterpart IM-DD system. The optimal polarization angle is independent of optical wavelengths and fiber distances, so it can be easily applied in wavelength-division-multiplexing (WDM) systems. In our experiment, 100-Gbps, 84-Gbps, 68-Gbps, 58-Gbps and 52-Gbps PAM-4 signals are successfully transmitted by our PolM-DD system over distances of 5-km, 10-km, 15-km, 21-km and 25-km SSMF, respectively, without dispersion compensation component or single sideband (SSB) modulation. The experimental results are consistent with our analysis and simulations results, and support more than 41% data rate gain compared to the IM-DD system, given comparable component bandwidths.**

***Index Terms*—Polarization modulator, tunable frequency response, optical communication**

I. Introduction

HE GaAs-based polarization modulator (PolM) is combined with two birefringent crystals and a half-wave plate to produce polarization modulation of incident light beam and exhibits the unique characteristic of simultaneous intensity and complementary phase modulations [1, 2]. As an extension of the Mach-Zehnder modulators (MZMs), the polarization modulator was initially studied as a polarization converter [3-5]. The PolM is a special phase modulator that can support both transverse-electric (TE) and transverse-magnetic (TM) modes with opposite phase modulation indices. By controlling the incident lightwave with a pair of polarization controllers (PCs), the two phase-modulated signals can be combined to generate an intensity-modulated signal. A 40-GHz PolM was first introduced in 2004 [6] with low differential group delay, on the order of a few tens of femto-seconds, and low driving voltage, on the order of 5 V. Later, PolMs were used as intensity modulators and over the past two decades have been widely studied in conjunction with microwave photonics (MWP) to improve the information and telecommunication systems. Before 2010, one promising application of PolMs was frequency-doubling optoelectronic oscillators (OEOs) [7-9]. Compared to the bias-drifting problem of the MZM-based OEOs, the PolM system is controlled by a pair of PCs. Almost at the same time, a simple approach to generate negative coefficients in a photonic microwave delay-line filter using a PolM was proposed [10-12]. In recent years, more practical applications of PolMs are studied in the fields of photonic-assisted microwave channelizers [13, 14], Doppler frequency shift estimations [15, 16], angle-of-arrival measurements [17], phase noise measurements [18] and ultra-wide band signal generators [19, 20].

The continuous increase of bandwidth hungry services such as cloud computing, high-definition live TV and online games have stimulated the requirements of high-speed communications [21]. Low-cost and high-speed communications are greatly desired by the upcoming 5G mobile fronthaul networks, especially Fronthual I transmissions between the distributed unit (DU) and the remote radio unit (RRU), whose distances usually range from 0 to 20 km. The direct-detection scheme stands out because of its lower cost compared to the coherent detection and simplicity but with the loss of phase state-of-polarization information. Intensity double

This paragraph of the first footnote will contain the date on which you submitted your paper for review. It will also contain support information, including sponsor and financial support acknowledgment. For example, "This work was supported in part by the U.S. Department of Commerce under Grant BS123456."

S. Liu and H. Tian are with the State Key Laboratory of Information Photonics and Optical Communications, School of Information and Telecommunication Engineering, Beijing University of Posts and Telecommunications, Beijing 100876, China (e-mail: hptian@bupt.edu.cn).

P.-C. Peng is with the Department of Electro-Optical Engineering, National Taipei University of Technology, Taipei, Taiwan.

L. Huang, C.-W Hsu and G.-K. Chang are with the School of Electrical and Computer Engineering, Georgia Institute of Technology, Atlanta, GA, 30308 USA (email: gkchang@ece.gatech.edu).

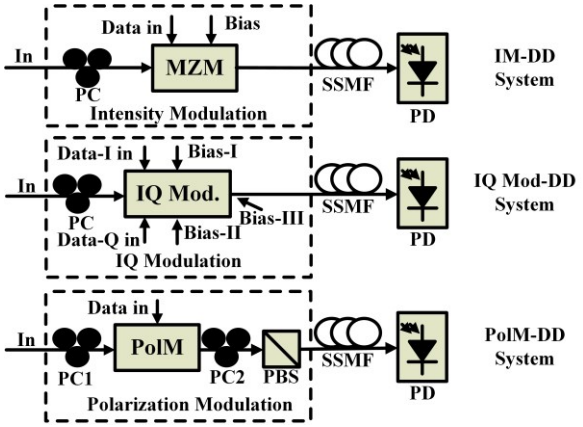

Fig. 1. Structures of different kinds of direct-detection transmission schemes.

sideband (DSB) modulation is the simplest scheme with which to upload an electrical signal onto an optical carrier by using a single-drive MZM. However, due to the chromatic dispersion (CD) induced by fibers, the optical carrier and its sidebands are transmitted along the fiber at different velocities and, thus have different phase. The double sideband beating with different phase causes power fading effect, which greatly degrades the signal quality [22, 23]. To solve this problem, many researchers have focused on single sideband (SSB) modulation which strongly depends on narrow band optical filters or dual-drive MZMs and suffers from signal-to-signal beat interferences (SSBI) [24]. The PolM can perform simultaneous amplitude and phase modulations and the ratio between the two can be adjusted by changing the polarization state of the optical signals injected into the modulator, which is later used to compensate the dispersion-induced power fading effect [25]. Up to now, most of the transmission work related to PolMs focused on radio-over-fiber (RoF) systems and the bitrates are about 1 Gbit/s [26-31]. Baseband transmission using PolMs is also reported in a wavelength-division-multiplexing passive optical network (WDM-PON). A 10-Gbps re-modulation scheme with downstream polarization shift-keying coded by a PolM and upstream on-off keying was demonstrated [32]. However, its potential for high-speed applications with a tunable frequency range, has not yet been experimentally demonstrated.

This paper is an extension of our recent work published by OFC 2018 [33]. In this paper, we firstly propose a bandwidth-enhanced PAM-4 polarization-modulation and direct-detection (PolM-DD) system at a wavelength around 1550 nm with a tunable frequency range after standard single mode fiber (SSMF) transmissions. By controlling the principal axis of the PBS to have an angle of α to one principal axis of the PolM, the peak frequency response can be shifted to the optimal position and the power fading effect around this frequency can be reduced. Comparisons between intensity-modulation and direct-detection (IM-DD) system with a single-drive MZM and PolM-DD system after SSMF transmissions illustrate that the proposed PolM-DD system is able to provide a wider available 3-dB bandwidth at baseband. Therefore, without dispersion compensation components, the PolM-DD system is able to transmit higher bitrate data over the same fiber distance compared to the IM-DD system. In the proposed PolM-DD system, some digital signal processing (DSP) techniques such as, time-domain least mean square (LMS) pre-equalization at transceiver and linear LMS, nonlinear Volterra-series post-equalizations and maximum likely sequence estimation Viterbi (MLSE-Viterbi) decoding at the receiver are employed to improve the system performances. Experimental results demonstrate that the proposed PolM-DD system successfully transmits 100-Gbps, 84-Gbps, 68-Gbps, 58-Gbps and 52-Gbps PAM-4 signals through 5-km, 10-km, 15-km, 21-km and 25-km SSMF for a forward error correction (FEC) bit error rate (BER) threshold of 3.8×10^{-3} without dispersion compensation components, respectively. In Section II, we theoretically demonstrate the features of a PolM and make comparisons between the proposed PolM-DD and traditional IM-DD systems. Section III introduces our experimental test bed with a PolM. Section IV summarizes the experimental results and data analysis. Finally, Section V provides concluding remarks and suggests future work.

II. Theoretical Analysis of the PolM-DD System

Direct detection stands out by its easy implementations and low expense compared to the coherent-detection scheme, which makes it the most popular detection scheme in wideband communication systems. Fig. 1 gives the simple diagrams of the IM-DD, IQ modulation direct-detection (IQ Mod-DD) and PolM-DD systems. The first IM-DD system is the most commonly used one to modulate signals onto optical carriers using a single-drive Mach-Zehnder modulator (MZM). This scheme suffers from power fading effects induced by fiber dispersion and the MZM must be biased at its quadrature point with the bias-shifting problem. To solve the power fading problem, many researchers have focused on the SSB modulations generated by an IQ modulator or a dual-drive Mach-Zehnder modulator (DDMZM). A DDMZM consists of two parallel phase modulators (PMs) which are driven with a bias difference of $V_\pi/2$ to achieve the function of IQ modulations. For the generation of SSB signals, the data in the Q branch should be the Hilbert pair of the data in the I branch and the two should be strictly synchronized [34]. To make the IQ modulation stable, usually a specially designed bias-control circuit and a pair of phase-controlled waveguides are required, which greatly increase the cost of the transmitter. Some other SSB signal generation schemes, such as the ones using narrow-band optical filters, also increase the system complexity and the signals suffer from SSBI [24]. The PolM-DD system has a tunable frequency response controlled by the second PC shown in Fig. 1, endowing it with the ability to mitigate the power fading limitations caused by CD. The bias power supply is not necessary because the modulation curve can be controlled by the two PCs, therefore, the polarization modulation module, including a PolM, a pair of PCs and a polarization beam splitter (PBS), is completely passive and it does not need a source of power such as MZM drivers. The state of polarization in our experimental configuration is sensitive to drift, but this drift can be either mitigated by system-in-package component integration or photonic integrated circuits when that technology achieves a higher manufacturing yield.

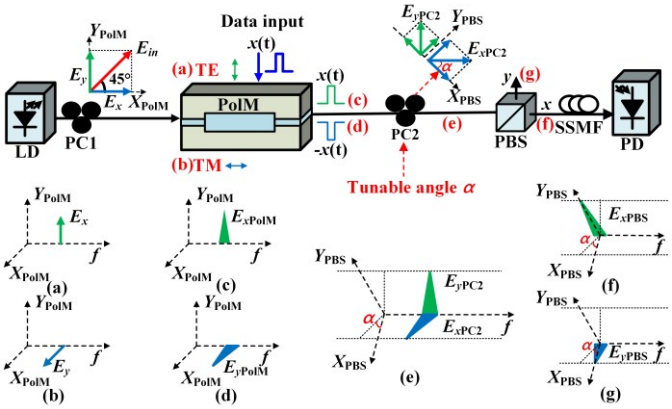

Fig. 2. Schematic diagram of the PolM-DD system.

The proposed PolM-DD system is schematically shown in Fig. 2. The PolM is equivalent to a special phase modulator that can support both TE and TM modes with opposite phase modulation indices [1]. By controlling PC1 before the PolM, a linearly polarized incident light is oriented to an angle of 45° to one principal axis of a PolM and then, complementary phase modulation signals are generated along the two principal axes. The normalized optical field at the output of the PolM along the two polarization axes can be expressed as

$$\begin{bmatrix} E_{xPolM}(t) \\ E_{yPolM}(t) \end{bmatrix} = \frac{\sqrt{2}}{2}\begin{bmatrix} \exp[j\omega_c t + j\gamma\phi(t) + j\varphi_0] \\ \exp[j\omega_c t - j\gamma\phi(t)] \end{bmatrix} \tag{1}$$

where ω_c is the angular frequency of the optical carrier, γ is the phase modulation index and takes on values from 0 to 1, and $\phi(t)$ is the modulated signal. φ_0 is the phase difference between $E_{xPolM}(t)$ and $E_{yPolM}(t)$ and this difference can be changed by adjusting the PC1 placed before the PolM. The second PC2 is adjusted to align the polarization direction of light emerging from PolM so as to make the angle α with respect to the principal axis of the PBS. Suppose we use port x of the PBS as the output of the modulation module, then we have

$$\begin{aligned} E_{xPBS}(t) &= \frac{\sqrt{2}}{2}\{\cos\alpha\exp[j\omega_c t + j\gamma\phi(t) + j\varphi_0] + \sin\alpha\exp[j\omega_c t - j\gamma\phi(t)]\} \\ &= \frac{\sqrt{2}}{2}\exp(j\omega_c t)[\cos\alpha\exp(j\varphi_0/2)\cos(\gamma\phi(t) + \varphi_0/2) \\ &\quad + (\sin\alpha - \cos\alpha)\exp(-j\gamma\phi(t))] \end{aligned} \tag{2}$$

As shown in Eq. (2), the lightwave is intensity- and phase-modulated simultaneously, which is equivalent to an intensity modulation with a tunable chirp controlled by adjusting the angle α. The lightwave is transmitted only in one polarization state and insensitive to polarization-mode dispersion (PMD). Suppose the PolM is modulated by a single-frequency sinusoidal signal with a zero initial phase

$$\phi(t) = \cos(\omega_m t) \tag{3}$$

where ω_m is the angular frequency of the modulation signal. Assume that the dispersive device has a unity magnitude response but a quadratic phase response, the optical signal at the output of the SSMF can be expressed as [25]

$$\begin{aligned} E_{out}(t) &= \frac{\sqrt{2}}{2}\exp(j\omega_c t)\{J_0(\gamma)(\exp(j(\varphi_0 + \theta_0))\cos\alpha + \exp(j\theta_0)\sin\alpha) \\ &+ J_1(\gamma)\cos\alpha(\exp j(\omega_m t + \frac{\pi}{2} + \varphi_0 + \theta_{+1}) - \exp j(-\omega_m t - \frac{\pi}{2} + \varphi_0 + \theta_{-1})) \\ &+ J_1(\gamma)\sin\alpha(\exp j(\omega_m t + \frac{3\pi}{2} + \theta_{+1}) - \exp j(-\omega_m t - \frac{3\pi}{2} + \theta_{-1}))\} \end{aligned} \tag{4}$$

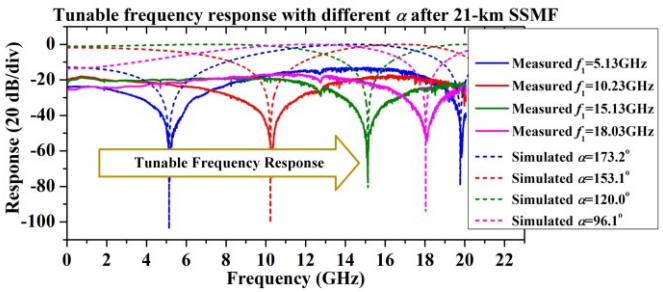

Fig. 3. Tunable frequency response of the PolM-DD system after 21-km SSMF transmissions with a variable angle of α.

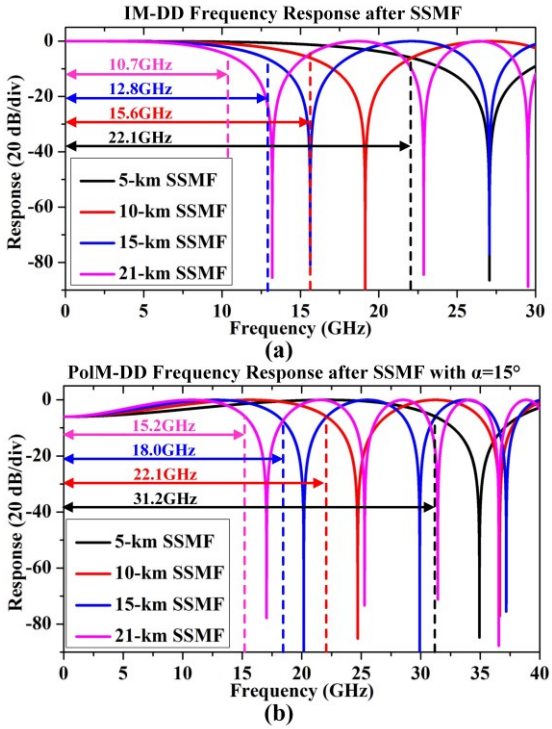

Fig. 4. Theoretical 3-dB bandwidth limit of the (a) IM-DD system and (b) PolM-DD system at baseband over different fiber distances.

where $J_n(\gamma)$ denotes the nth-order Bessel function of the first kind, θ_0, θ_{+1} and θ_{-1} are the phase shifts that are experienced by the optical carrier, the upper sideband and the lower sideband, respectively.

In general, the phase shift introduced by a dispersive device, usually fiber, can be expressed as $\theta(\omega)=\beta(\omega)z$, where $\beta(\omega)$ is the propagation constant and z is the fiber distance. The second-order Taylor series of $\beta(\omega)$ near the optical frequency ω_c can be expressed as:

$$\theta(\omega) \approx z\beta(\omega_c) + z\beta'(\omega_c)(\omega - \omega_c) + \frac{1}{2}z\beta''(\omega_c)(\omega - \omega_c)^2 \tag{5}$$

where $\beta'(\omega_c)$ and $\beta''(\omega_c)$ are the first- and second-order derivatives of $\beta(\omega_c)$ with respect to the optical angular frequency. Then let $\omega=\omega_c+\omega_m$, $\omega=\omega_c$ and $\omega=\omega_c-\omega_m$, we have

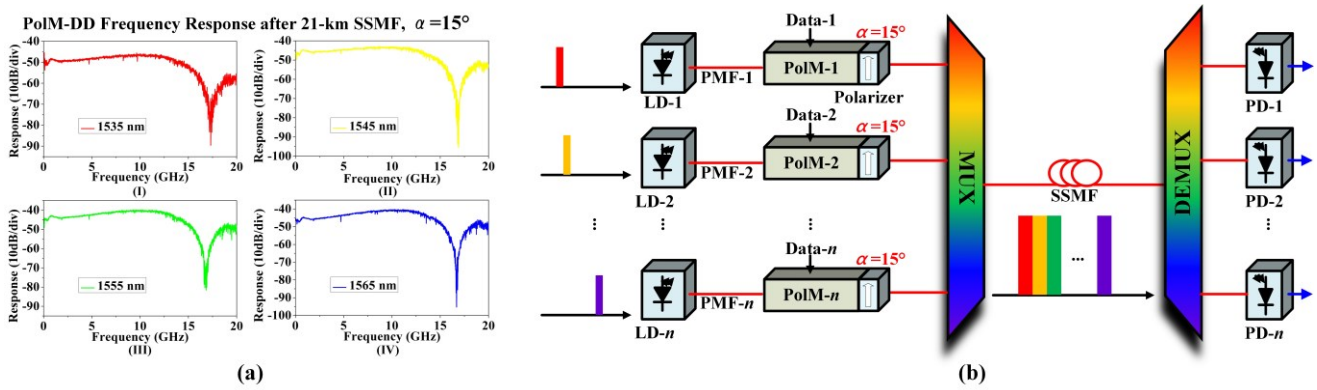

Fig. 5(a) Measured electrical spectrum of the PolM-DD channels at different wavelengths. (b) Schematic of the WDM system based on polarization modulations. PMF: polarization maintaining fiber, LD: laser diode, PolM: polarization modulator. MUX: multiplexer, DEMUX: de-multiplexer.

$$\begin{cases} \theta_{+1} = z\beta(\omega_c) + z\beta'(\omega_c)\omega_m + \frac{1}{2}z\beta''(\omega_c)\omega_m^2 \\ \theta_0 = z\beta(\omega_c) \\ \theta_{-1} = z\beta(\omega_c) - z\beta'(\omega_c)\omega_m + \frac{1}{2}z\beta''(\omega_c)\omega_m^2 \end{cases} \tag{6}$$

After a square-law photo detector (PD) and ignoring the unnecessary frequency components, the photo current is shown as follow:

$$i_{PD} \propto |E_{out}(t)|^2 = 2J_0J_1[\sin 2\alpha \cos(\frac{1}{2}z\beta''(\omega_c)\omega_m^2)\sin\varphi_0 + \cos 2\alpha \sin(\frac{1}{2}z\beta''(\omega_c)\omega_m^2)]\cos[\omega_m(t-\tau_0)] \tag{7}$$

By controlling PC1, the phase difference can be adjusted to $\varphi_0=\pi/2$, and Eq. (7) can be written as

$$i_{PD} \propto 2J_0J_1 \sin(2\alpha + \frac{1}{2}z\beta''(\omega_c)\omega_m^2)\cos[\omega_m(t-\tau_0)] \tag{8}$$

The definition of group delay is the derivative of phase shift. Near the optical frequency ω_c, the delay can be expressed as:

$$\tau(\omega) = \frac{d\theta(\omega)}{d\omega} = z\beta'(\omega_c) + z\beta''(\omega_c)(\omega-\omega_c) \tag{9}$$

In Eq. (9), the first term group delay is $\tau_0=z\beta'(\omega_c)$ at the optical carrier frequency ω_c. Considering the definition of the fiber dispersion parameter, it should be the partial derivative of group delay $\tau(\omega,z)$ with respect to optical wavelength λ and fiber distance z, we get

$$D(\lambda_c) = \left|\frac{\partial\tau(\omega,z)}{\partial\lambda\partial z}\right|_{\lambda=\lambda_c} = \left|\frac{\partial}{\partial\lambda}[\beta'(\omega_c)+\beta''(\omega_c)(\omega-\omega_c)]\right|_{\lambda=\lambda_c} = \frac{\omega^2}{2\pi c}\frac{\partial}{\partial\omega}[\beta''(\omega_c)(\omega-\omega_c)]\Big|_{\omega=\omega_c} = \frac{\omega^2\beta''(\omega_c)}{2\pi c}\Big|_{\omega=\omega_c} = \frac{\omega_c^2\beta''(\omega_c)}{2\pi c} \tag{10}$$

Substituting Eq. (10) into Eq. (8) and replacing the $\beta''(\omega_c)$ by the dispersion parameter $D(\lambda_c)$, we arrive at an expression for the frequency response of the PolM-DD system,

$$H_{PolM-DD}(\omega_m) = \sin(2\alpha + \frac{1}{2}z\beta''(\omega_c)\omega_m^2) = \sin(2\alpha + \frac{\pi czD(\lambda_c)\omega_m^2}{\omega_c^2}) \tag{11}$$

As a result, a tunable frequency response is obtained by varying the angle α in Eq. (11) through controlling PC2 before the PBS.

To verify the theory discussed above, simulated and measured frequency responses of the PolM-DD system are given in Fig. 3. In the measurement, we define the frequency of the first notch to be f_1. By tuning the PC2 in the system, f_1 is shifted from 5.13 GHz to 18.03 GHz. In the simulations, the parameters in Eq. (11) are λ_c=1552.6 nm, c=3×10^8 m/s, z=21 km and $D(\lambda_c)$=17 ps/(km·nm). As illustrated in Fig. 3, when the angle α equals to 173.2°, 153.1°, 120.0° or 96.1°, the simulated curve closely matches the measured frequency response of the system.

Since we have a tunable frequency response in the PolM-DD system according to the theoretical simulated and measured results given above, we can shift the first notch f_1 from lower to higher frequency positions, thus a wider available 3-dB bandwidth can be obtained at baseband. The tunability of frequency response makes it more suitable for high-speed communications with simple modulation formats at baseband such as PAM-4 signals compared to the IM-DD system. Fig. 4(a) shows the theoretical 3-dB bandwidth limit of the IM-DD system at baseband for different fiber propagation distances, which are calculated by

$$H_{IM-DD}(\omega_m) = \cos(\frac{\pi czD(\lambda_c)\omega_m^2}{\omega_c^2}) \tag{12}$$

The parameters are as defined above. From Eq. (12), we can obtain the 3-dB bandwidths as

$$\omega_{IM-3dB} = \sqrt{\arccos(\frac{1}{2})\frac{\omega_c^2}{\pi czD(\lambda_c)}} \tag{13}$$

Fig. 4(b) shows the maximum available 3-dB bandwidth of the PolM-DD system at the baseband. In order to shift the first notch to higher frequency positions as much as possible, when ω_m=0 or DC, the normalized frequency response should be $H_{PolM-DD}(0)$=-3 dB, thus we have $\alpha=\pi/12=15°$. Then, the 3-dB bandwidth in the PolM-DD system is obtained by

$$\omega_{PolM-3dB} = \sqrt{[\arcsin(\frac{1}{2}) - 2\alpha]\frac{\omega_c^2}{\pi czD(\lambda_c)}} \tag{14}$$

Theoretical comparisons between the IM-DD and PolM-DD systems based on baseband 3-dB bandwidths demonstrate that the PolM-DD system has about 41.4% more available 3-dB baseband bandwidth than the IM-DD system. Especially when transmitting through 5-km SSMF, by changing the angle α to 15°, the first frequency notch is shifted to the frequency near 35 GHz, leaving a 31.2-GHz 3-dB bandwidth at the lower frequency, which is wide enough to realize 100-Gbps PAM-4 transmissions without the help of dispersion compensation or

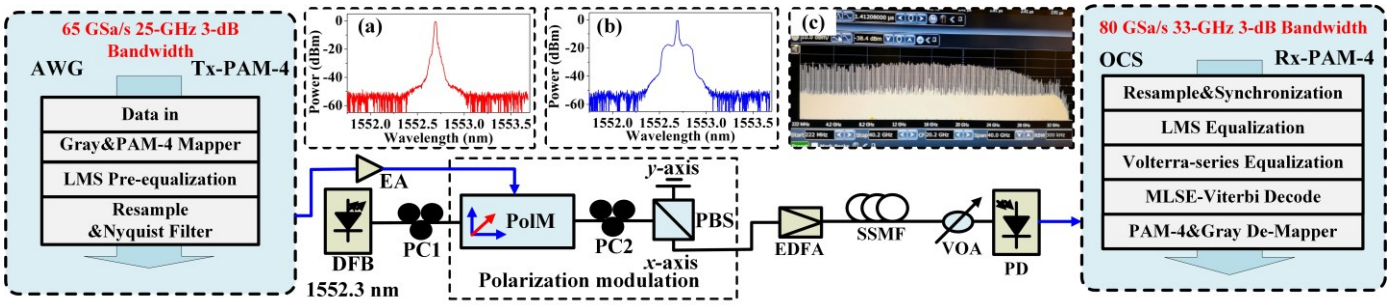

Fig. 6. Experimental setup of the 100-Gbps PAM-4 PolM-DD system. Insets (a) and (b) are the optical spectrum before PD without and with PAM-4 signal modulations. Inset (c) is the electrical spectrum of the multi-tone signal after PD. AWG: arbitrary waveform generator, EA: electrical amplifier, DFB: distributed feedback laser, PC: polarization controller, PolM: polarization modulator, PBS: polarization beam splitter, EDFA: Erbium doped fiber amplifier, SSMF: standard single mode fiber, VOA: variable optical attenuator, PD: photo detector, OCS: oscilloscope.

SSB modulation. However, for the IM-DD system, the 3-dB bandwidth through 5-km SSMF is about 22.1 GHz and it is not sufficient to realize 100-Gbps PAM-4 transmissions. As far as we know, there exists no published report on a 100-Gbps PAM-4 IM-DD system successfully transmitting through 5-km SSMF without dispersion compensation component or SSB modulation at wavelength around 1550 nm. What's more, because the PolM-DD system has a tunable frequency response, when transmitting intermediate frequency signals, such as OFDM or M-QAM over SSMF, we can adjust the angle α to other angle to get the best signal quality.

With different angle α, the extinction ratio of the modulator changes. According Eq. (2), when $\alpha=\pi/12$, the intensity modulation section of the optical signal becomes a little smaller, the index of intensity modulation deviates from its maximal value 1 to $\cos(\pi/12)\approx0.97$. Therefore, the designed scheme achieves the optimal frequency response at the expense of decreasing extinction ratio, but not too much.

In order to verify the dependence of the frequency response on the wavelength, we test the PolM-DD channel through *C*-band. Fig. 5(a) shows the frequency response at the wavelengths of 1535 nm, 1545 nm, 1555 nm and 1565 nm. The small variation in the response curves can be ascribed to small variations in the dispersion parameter $D(\lambda_c)$. According to the analysis above, the optimal polarization angle α can be 15°, independent of wavelength position and fiber distance. While in the case of IM-DD system, it is necessary to change the dispersion compensation components as the wavelength changes. Fig. 5(b) shows the potential applications of PolM-DD systems in a WDM system. For the long-term stability, the PCs can be replaced by polarization maintaining fibers (PMF). The polarizers are designed to have a 15° discrepancy between one principal axis of the PolMs. Considering the WDM module with multiple PolMs, one polarizer can be set to the location after the multiplexer (MUX) to replace the multiple polarizers integrated at the output of the PolMs before the MUX, further decreasing the cost of manufacture.

III. Experimental Setup

Fig. 6 describes the experimental setup used to verify the performance of the proposed high-speed PAM-4 PolM-DD system. Electrical baseband signals are generated by an arbitrary waveform generator (AWG) with a sampling rate of 65 GSa/s and a 3-dB bandwidth of 25 GHz. After Gray code and PAM-4 mapping, a LMS pre-equalizer with 100 symbol-duration delay taps is applied to adjust the uneven channel frequency response. Before injected into the PolM, the signals are resampled and passed through Nyquist filter to increase the frequency efficiency. After that, the signals generated by the AWG are injected into a 40-GHz PolM without bias power. The PolM is a model PL-40G-5-1550 from Versawave Technologies Inc. [6]. The distributed feedback laser (DFB) with a center wavelength at 1552.3 nm is followed by PC1, which is used to align the polarization direction of the incident light so as to make an angle of 45° with respect to one principal axis of the PolM. PC2 is used to adjust the angle α between the principal axis of the PBS and PolM. After transmissions over 5-km to 25-km SSMF, the optical signals are sent to a PD with a responsivity of 0.65 A/W and a 3-dB bandwidth of 65 GHz. Finally, a digital oscilloscope (OCS) running at sampling rate 80 GSa/s captures the signals. The received signal is further processed offline using DSP software available in Matlab. The post-LMS linear and Volterra-series nonlinear equalizations are employed to enhance the signal quality. The tap number in linear LMS equalizer is 100 while the tap number and nonlinear order of the Volterra-series nonlinear equalizer are 3 and 3, respectively. Then a soft-decision MLSE-Viterbi decoder with a trace-back length of 10 and a memory length of 4 is used to further increase the BER performance. In the experiments, 10% data in the sequence is used as training data to get the coefficients of equalizers and channel information.

IV. Experimental Results

Fig. 7 shows the experimental frequency response of the 5-km SSMF PolM-DD system with different polarization angles α. The first column in Fig. 7 is the frequency response of multi-tone signals which have identical power at each tone, and the 100 tones are equally distributed from 300 MHz to 30 GHz with 300 MHz frequency interval spacing. The power fading effect can be easily observed from the spectrum of received multi-tone signals. The second and third columns in Fig. 7 are the spectra of the 100-Gbps PAM-4 signals without and with pre-equalization at the transmitter. The frequency spectrum in each row has the same polarization angle α and the notches caused by CD in SSMF are located at the same frequency position. As illustrated in the 4th row of Fig. 7, with properly controlled

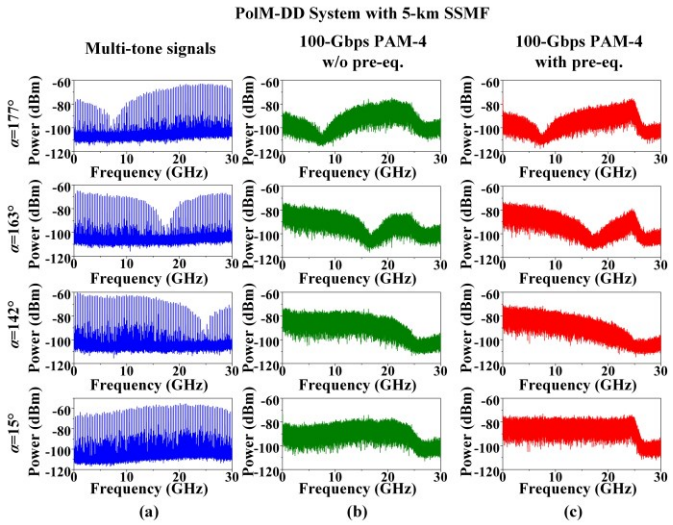

Fig. 7. Frequency response of the PolM-DD system with varying polarization angles α when transmitting (a) 30-GHz multi-tone signals with 300-MHz intervals, (b) 100-Gbps PAM-4 signals without pre-equalizations, (c) 100-Gbps PAM-4 signals with pre-equalizations

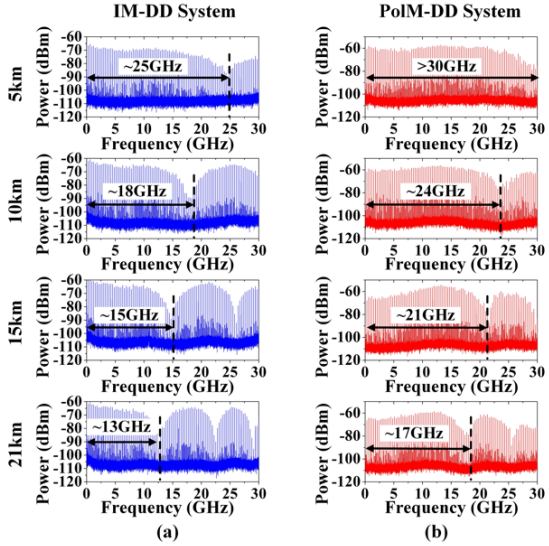

Fig. 8. Frequency response of the multi-tone signals when transmitting through a (a) IM-DD system and (b) PolM-DD system with varying fiber distances.

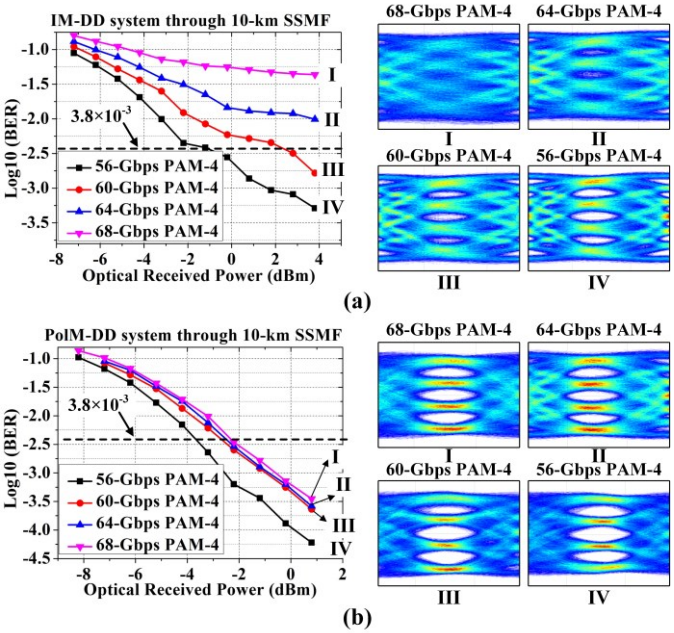

Fig. 9. BER performances and eye diagrams of the received PAM-4 signals in (a) IM-DD system and (b) PolM-DD system through 10-km SSMF with different bitrates.

angle α, the first notch can be shifted to the frequency higher than 30 GHz, which is out of the BW scale of our OCS. These results verify the theoretical analyses and simulations shown in Section II, where we have discovered that the first notch can be shifted to nearly 35 GHz with a 3-dB bandwidth greater than 31 GHz. However, the frequency response of the channel within the 3-dB bandwidth is not flat. This phenomenon causes critical inter-symbol interferences in channels. Therefore, LMS pre-equalization is employed and a very flat spectrum of the PAM-4 signal is observed, indicating the feasibility of the 100-Gbps PAM-4 transmissions through 5-km SSMF in the proposed PolM-DD system.

Fig. 8 compares the multi-tone frequency response of the IM-DD and PolM-DD systems over different SSMF distances. The IM-DD system is tested by substituting a one-drive X-cut MZM for the polarization modulation module shown in Fig. 6. The X-cut MZM has a chirp parameter of 0 [35]. When the transmission distance increases from 5 km to 21 km, the available baseband bandwidth in the IM-DD system reduces from approximately 25 GHz to 13 GHz. The attenuation at the frequency notch caused by CD in SSMF is too large to be recovered by LMS pre-equalizations. As seen in Section II, through a 5-km SSMF, the available 3-dB bandwidth for the IM-DD system at baseband is about 22.1 GHz, making it difficult to realize 100-Gbps PAM-4 transmissions without the help of dispersion compensation components. While for the PolM-DD system, the baseband bandwidth is much higher.

In order to verify the feasibility of the proposed system, the BER performances of the two systems through 10-km of SSMF are given as a function of data rate. According to the simulations in Fig. 4(a), the 3-dB bandwidth at baseband in the IM-DD system is about 15.6 GHz and, in theory, it can support a 62.4-Gbps PAM-4 data stream. The BER performances in Fig. 9(a) verify this conclusion. When the bitrate is less than 60 Gbps, the PAM-4 signals in the IM-DD system is able to reach the FEC BER limit of 3.8×10^{-3}. However, when the bitrates reach 64 Gbps and 68 Gbps, which are higher than the 62.4 Gbps, the bandwidth of the PAM-4 signals are out of the 3-dB band of the channel and the BER performances greatly degrade. The degradation can also be seen from the progressive closing of the eye diagrams from IV to I in Fig. 9(a). In the case of PolM-DD system, the theoretical 3-dB bandwidth through 10-km SSMF is about 22.1 GHz, as shown in Fig. 4(b), which is much wider than its counterpart and can support 88.4-Gbps PAM-4 signals in the ideal case. The BER performances in Fig. 9(b) further verify the theory and demonstrate that increasing bitrate of the PAM-4 signals (up to 68 Gbps) has little influence on the signal quality because the PAM-4 signal bandwidths are still in the 3-dB bandwidth of PolM-DD system. When the PAM-4 bitrate reaches 68-Gbps, the eye is still open, as demonstrated by the

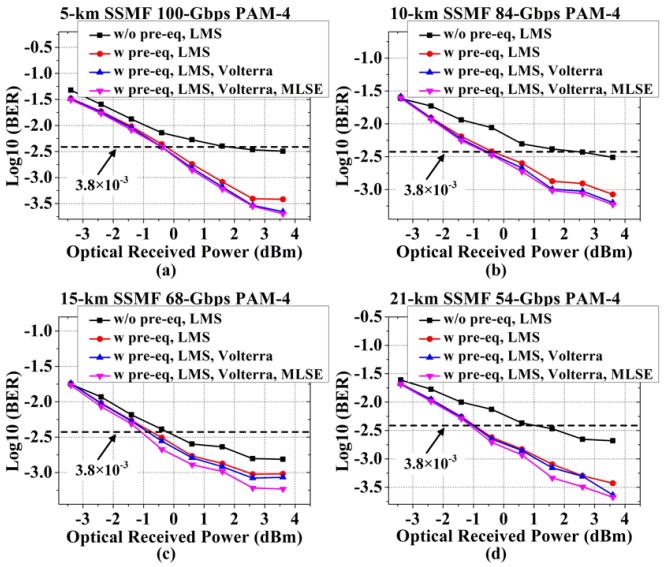

Fig. 10. BER performances of the proposed PolM-DD system as functions of received power over different fiber distances.

eye diagram IV in Fig. 9(b).

Fig. 10 shows the BER performances of the PolM-DD system as functions of the optical received power with varying transmission distances. As calculated from the bandwidths in Fig. 4, the theoretical bitrate limits for PAM-4 signals through 5-km, 10-km, 15-km and 21-km SSMF can be expected to be, in the ideal PolM-DD system, 124.8 Gbps, 88.4 Gbps, 72.0 Gbps and 60.8 Gbps, respectively. In the experiment, we successfully transmit 100-Gbps, 84-Gbps, 68-Gbps and 54-Gbps PAM-4 signals through 5-km, 10-km, 15-km and 21-km SSMF, which is consistent with our analysis. In the 5-km SSMF case, the PAM-4 signals are limited by the bandwidth of the experimental equipment (mainly the bandwidth of AWG which is limited to 25 GHz). The influences of the LMS linear pre- and post-equalizers, the Volterra-series nonlinear equalizer and MLSE-Viterbi decoder are also studied. The post-LMS linear equalizer is the most important equalizer in the experiment, because the frequency response in the PolM-DD system fluctuates, mainly due to the CD in the fiber and the imperfect frequency response of the device. Without the LMS equalizer, the eye diagrams of the signals are completely closed. The LMS pre-equalizations at the transmitter also greatly enhance system BER performances by increasing the signal-to-noise ratio (SNR) at the low-power frequency response positions, especially when the data rate is high, such as 100 Gbps. The static phase shift φ_0=0, π/2 and π in Eq. (1) corresponds to the biasing points in a MZM at the maximum transmission point, quadrature point and the minimum point, respectively. A non-ideal polarization direction is the one in which φ_0 is off the quadrature point and may introduce some nonlinearities to the signals. Therefore, Volterra-series nonlinear equalizer is also employed to eliminate the possible effects due to the nonlinear impairments in channel. Finally, to take the full advantage of the correlation in signals, MLSE-Viterbi decoder is used to further increase the signal quality.

Fig. 11 shows the data rate limitations of the IM-DD and PolM-DD systems as functions of fiber distances. The

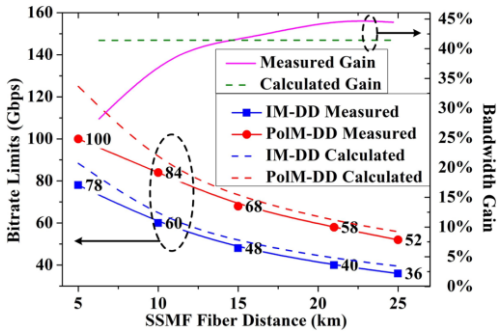

Fig. 11. Speed limits of IM-DD and PolM-DD systems with varying fiber distances.

theoretical limits of the two kinds of systems are given by the 3-dB bandwidths before the first notch. For the measured results, the upper BER limit is taken, at per convention, at 1×10^{-3}. From the theoretical curves in Fig. 11, the bandwidth gain of the PolM-DD over the IM-DD system is statically maintained at 41.4%, while the measured results indicate bandwidth gain from 28.2% to 44.4%. When transmitting the 100-Gbps PAM-4 signals through PolM-DD system with a 5-km SSMF, fiber chromatic dispersion is no longer the dominant impediment, rather, the system becomes limited by our experimental equipment.

V. Conclusions

In this paper, we have demonstrated, for the first time, how to construct a simple baseband bandwidth-enhanced PAM-4 PolM-DD transmission system with a tunable frequency range to mitigate the power fading effect at baseband. The power fading effect is caused by the CD in SSMF and greatly limits the transmission bandwidth and distance. In polarization modulations, the interplay between the intensity and phase modulations changes the fading effect and makes the channel response tunable. The proposed system transmits signals in one polarization state and is immune to PMD. Compared to the IM-DD and IQ Mod-DD systems, the PolM-DD system has the advantage of no bias requirements and easy implementations. In the system reported here, when the angle α between the principal axis of the PBS and one principal axis of the PolM equals to 15°, the largest available 3-dB bandwidths at baseband attains irrespective of fiber distance and optical wavelength. We have also calculated that PolM-DD system has a 3-dB baseband bandwidth approximately 41% wider than the traditional IM-DD system. Considering the optimal angle α is independent of optical wavelengths and transmission distances, the system is also applicable to WDM transmissions. Comparisons between the PolM-DD and IM-DD schemes on the multi-tone frequency response testing demonstrate the bandwidth advantage of the proposed PolM-DD system. Finally, we have transmitted high-speed PAM-4 signals through the two systems. The data rate limits are obtained both theoretically and experimentally. Through 5-km, 10-km, 15-km, 21-km and 25-km SSMF transmissions, the PolM-DD system successfully transmitted 100-Gbps, 84-Gbps, 68-Gbps, 58-Gbps and 52-Gbps PAM-4 signals under the BER of 1×10^{-3} without dispersion compensation component, while for the IM-DD

system, only 78-Gbps, 60-Gbps, 48-Gbps, 40-Gbps and 36-Gbps PAM-4 can be similarly obtained. The experimental results are in good agreement with the simulation results and support the feasibility of the PolM-DD system.

The PolM-DD-based bandwidth-enhanced communication system is a potential candidate for the Tie-I 5G mobile fronthaul networks due to the employment of low-cost components, no need for dispersion compensation, insensitive to operation wavelengths in *C*-band and a larger usable coverage range, at least up to 25-km SSMF.

ACKNOWLEDGMENT

This work was supported in part by the NSF I/UCRC Center of Fiber-Wireless Integration and Networking (FiWIN), by NSFC under Grant No. 61372038, and 61431003, the project of Joint Laboratory for Undersea Optical Networks, China.

REFERENCES

[1] X. Zou and J. Yao, "Repetition-rate-tunable return-to-zero and carrier-suppressed return-to-zero optical pulse train generation using a polarization modulator". *Opt. Lett.*,vol. 34, no. 3, pp. 313-315, Feb. 2009.

[2] Y. Xiang and S. Pan, "GaAs-based polarization modulators for microwave photonic applications," *Front. Optoelectron.*, vol. 9, no. 3, pp. 497-507, Sep. 2016.

[3] F. Rahmatian, N. A. F. Jaeger, R. James and E. Berolo, "An ultrahigh-speed AlGaAs-GaAs polarization converter using slow-wave coplanar electrodes," *IEEE Photo. Techno. Lett.*, vol 10, no. 5, pp. 675-677, May 1998.

[4] N. Grossard, H. Forte, J. –P Vilcot, B. Beche and J. –P. Goedgebuer, "AlGaAs-GaAs polarization converter with electrooptic phase mismatch control," *IEEE Photo. Techno. Lett.*, vol. 13, no. 8, pp. 830-832, Aug. 2001.

[5] H. Gnauck, J. Leuthold, C. Xie, I. Kang, S. Chandrasekhar, P. Bernasconi, C. Doerr and L. Buhl, "6×42.7-Gbps transmission over ten 200-km EDFA-amplified SSMF spans using polarization-alternating RZ-DPSK," in *Proc. Opt. Fiber Commun. Exhib.*, Los Angeles, CA, USA, 2004, paper. PDP35.

[6] J. D. Bull, N. A. F. Jaeger, H. Kato, M. Fairbum, A. Reid, P. Ghanipour, "40 GHz electro-optic polarization modulator for fiber optics communications systems," in *Proceedings of the Society for Photo-Instrumentation Engineers*, Ottawa, Ontario, Canada, 2004, pp. 133-143.

[7] S. Pan and J. Yao, "A frequency-doubling optoelectronic oscillator using a polarization modulator," *IEEE Photo. Techno. Lett.*, vol. 21, no. 13, pp. 929-931, Jul. 2009.

[8] S. Pan and J. Yao, "Optical clock recovery using a polarization-modulator-based frequency-doubling optoelectronic oscillator," *J. Lightwave Technol.*, vol. 27, no. 16, pp. 3531-3539, Aug. 2009.

[9] Z. Tang, S. Pan, D. Zhu, R. Guo, Y. Zhao, M. Pan, D. Ben and J. Yao, "Tunable optoelectronic oscillator based on a polarization modulator and a chirped FBG," *IEEE Photo. Techno. Lett.*, vol. 24, no. 17, pp. 1487-1489, Sep. 2012.

[10] J. Yao and Q. Wang, "Photonic microwave bandpass filter with negative coefficients using a polarization modulator," *IEEE Photo. Techno. Lett.*, vol. 19, no. 9, pp. 644-646, May 2007.

[11] J. Yao, "Microwave Photonics," *J. Lightwave Technol.* vol. 27, no. 3, pp. 314-335, Feb. 2009.

[12] Q. Wang and J. Yao, "Multitap photonic microwave filters with arbitrary positive and negative coefficients using a polarization modulator and an optical polarizer," *IEEE Photo. Techno. Lett.*, vol. 20, no. 2, pp. 78-80, Dec. 2008.

[13] X. Zou, W. Li, W. Pan, L. Yan and J. Yao, "Photonic-assisted microwave channelizer with improved channel characteristics based on spectrum-controlled stimulated Brillouin scattering". *IEEE T. Microw. Theory.*, vol. 61, no. 9, pp. 3470-3478, Jul. 2013.

[14] W. Li and J. Yao, "Dynamic range improvement of a microwave photonic link based on bi-directional use of a polarization modulator in a Sagnac loop," Opt. Express., vol. 21, no. 13, pp. 15692-15697, Jul. 2013.

[15] X. Zou, W. Li, B. Lu, W. Pan, L. Yan and L. Shao, "Photonic approach to wide-frequency-range high-resolution microwave/millimeter-wave Doppler frequency shift estimation," *IEEE T. Microw. Theory.*, vol. 63, no. 4, pp. 1421-1430, Apr. 2015.

[16] B. Lu, W. Pan, X. Zou, X. Yan, L. Yan and B. Luo, "Wideband Doppler frequency shift measurement and direction ambiguity resolution using optical frequency shift and optical heterodyning," *Opt. Lett.*, vol. 40, no. 10, pp. 2321-2324, May 2015.

[17] X. Zou, W. Li, W. Pan, B. Luo, L. Yan and J. Yao, "Photonicc approach to the measurement of time-difference-of-arrival and angle-of-arrival of a microwave signal," *Opt. Lett.*, vol. 37, no. 4, pp. 755-757, Feb. 2012.

[18] D. Zhu, F. Zhang, P. Zhou, D. Zhu and S. Pan, "Wideband phase noise measurement using a multifunctional microwave photonic processor," *IEEE Photo. Techno. Lett.*, vol. 26, no. 24, pp. 2434-2437, Dec. 2014.

[19] T. Shao and J. Yao, "Millimeter-wave and UWB over a colorless WDM-PON based on polarization multiplexing using a polarization modulator," *J. Lightwave Technol.*, vol. 31, no. 16, pp. 2742-2751, Aug. 2013.

[20] S. Pan and J. Yao, "UWB-over-fiber communications: modulation and transmission," *J. Lightwave Technol.*, vol. 28, no. 16, pp. 2445-2455, Aug. 2010.

[21] N. Eiselt, J. Wei, H. Griesser, A. Dochhan, M. Eiselt, J.-P Elbers, J. J. V. Olmos and I. T. Monroy, "First real-time 400G PAM-4 demonstration for inter-data center transmission over 100 km of SSMF at 1550nm," in *Proc. Opt. Fiber Commun. Exhib.*, Anaheim, CA, USA, 2016, paper W1K. 5.

[22] J. Ma, J. Yu, C. Yu, X. Xin, J. Zeng and L. Chen, "Fiber dispersion influence on transmission of the optical millimeter-wave generated using LN-MZM intensity modulation," *J. Lightwave Technol.*, vol. 25, no. 11, pp. 3244-3256, Nov. 2007.

[23] C. Lim, A. Nirmalathas, M. Bakaul, P. Gamage, Ka-Lun Lee, Y. Yang, D. Novak and R. Waterhouse, "Fiber-wireless networks and subsystem technologies," *J. Lightwave Technol.*, vol. 28, no. 4, pp. 1-16, Feb. 2010.

[24] Z. Li, M. S. Erkilinc, K. Shi, E. Sillekens, L. Galdino, B. C. Thomsen, P. Bayvel and R. I. Killey, "SSBI mitigation and Kramers-Kronig scheme in single-sideband direct-detection transmission with receiver-based electronic dispersion compensation," *J. Lightwave Technol.*, vol. 35, no. 10, 1887-1893, May 2017.

[25] H. Zhang, S. Pan, M. Huang, X. Chen, "Polarization-modulated analog photonic link with compensation of the dispersion-induced power fading," *Opt. Lett.*, vol. 37, no. 5, pp. 866-868, Mar. 2012.

[26] R. Li, W. Li, X. Chen and J. Yao, "Millimeter-wave vector signal generation based on a bi-directional use of a polarization modulator in a Sagnac loop," *J. Lightwave Technol.*, vol. 33, no. 1, pp. 251-257, Jan. 2015.

[27] T. Shao and J. Yao, "Millimeter-wave and UWB over colorless WDM-PON based on polarization multiplexing using a polarization modulator," *J. Lightwave Technol.*, vol. 31, no. 16, pp. 3042-3051, Aug. 2013.

[28] J. Zheng, H. Wang, L. Wang, N. Zhu, J. Liu and S. Wang, "Implementation of wave reusing upstream service based on distributed intensity conversion in ultrawideband-over-fiber system," *Opt. Lett.*, vol. 38, no. 7, pp. 1167-1169, Apr. 2013.

[29] R. Li, X. Han, X. Chen and J. Yao, "Vector signal generation using a polarization and phase modulator in a Sagnac loop," *IEEE Photo. Techno. Lett.*, vol. 27, no. 18, pp. 1961-1964, Sep. 2015.

[30] C. H. Chang, P. C. Peng, Q. Huang, W. Y. Yang, H. L. Hu, W. C. Wu, J. H. Huang, C. Y. Li, H. H. Lu and H. H. Yee, "FTTH and Two-band RoF Transport Systems Based on an Optical Carrier and Colorless Wavelength Separators," *IEEE Photonics J.*, vol. 8, no. 1, Article 7900308, Dec. 2016.

[31] P. C. Peng, L. H. Yen, C. H. Chang, Y. C. Chen and J. J. Jhang, "Hybrid wireline and wireless transport system based on polarization modulator," *IEEE Photo. Techno. Lett.*, vol. 25, no. 11, pp.1069-1072, Jun. 2013.

[32] R. Wang, S. Fu, P. P. Shum and C. Lin, "10 Gbit/s WDM-PON using downstream PolSK coded by polarization modulator and upstream intensity re-modulation," *Electrical Letter*, vol. 46, no. 6, pp. 428-430, Mar. 2010.

[33] S. Liu, P. C. Peng, C.-W. Hsu, H. Tian and G. K. Chang, "Realization of tunable frequency response in polarization modulation and direct detection scheme for high-speed optical access system," in *Proc. Opt. Fiber Commun. Exhib.*, San Diego, CA, USA, 2018, paper W4G.7.

[34] J. Shi, J. Zhang, Y. Zhou, Y. Wang, N. Chi and J. Yu, "Transmission performance comparison for 100-Gb/s PAM-4, CAP-16, and DFT-S OFDM with direct detection," *J. Lightwave Technol.*, vol. 35, no. 23, pp. 5127-5133, Dec. 2017.

[35] J. F. Diehl and V. J. Urick, "Chromatic dispersion induced second-order distortion in long-haul photonic links," *J. Lightwave Technol.*, vol. 34, no. 20, pp. 4646-4651, Oct. 2016.